DOI: 10.1002/ejic.201000221

Mg Environments in the Octahedral Sheet of 2:1 Talc-Like Hybrid Phyllosilicates: A Comparative XAFS Study

Jocelyne Miehé-Brendlé,[a] Marie-Hélène Tuilier,*[b] Claire Marichal,[a] Jean-Christophe Gallego,[a] and Marc Reinholdt[a][‡]

Keywords: Layered compounds / Talc / Montmorillonite / EXAFS spectroscopy

Phenethyl and Phenylaminomethyl talc-like hybrid (TLH) materials prepared by a one-step synthetic procedure are investigated by Mg *K*-edge X-ray absorption fine structure (XAFS) to obtain structural information on the octahedral sheet of these 2:1 phyllosilicates. A comparison of Mg *K*-edge X-ray absorption spectra of the talc-like hybrids, synthetic montmorillonite containing 20 % Mg and 80 % Al in the octahedral sheet, and MgO is presented. Three peaks are observed in the near-edge XAFS spectra of the phyllosilicates. Their interpretation is drawn from previous multiple scattering, band structure, and molecular cluster simulations of electron energy loss near-edge structures spectra of MgO. Among the theoretical approaches found in the literature, the molecular cluster calculations highlight the dependence of the observed features on Mg–O and Mg–Mg orbital overlaps. Our results reveal a lower Mg–Mg orbital overlap in the hybrid materials than in MgO. The extended XAFS analysis emphasises a deviation from the regular Mg octahedral coordination in the TLHs. Two different Mg–O distances are identified; the shorter one is found to be significantly higher than predicted in the theoretical talc structure.

Introduction

The 2:1 phyllosilicates have a lamellar structure made from stacking one octahedral (O) sheet of hexacoordinate atoms between two tetrahedral (T) sheets of tetracoordinate atoms. These materials can be functionalized in three ways:[1] by the intercalation of surfactant molecules by ion-exchange;[2] by the grafting of an organoalkoxysilane on silanol groups at the border of the layers;[3,4] or by one-step synthesis.[5–7] The third option enables new materials to be obtained with pendant organic moieties in the interlayer space that are covalently linked to the silicon atoms in the tetrahedral sheets. These solids are called organic–inorganic hybrids based on 2:1 phyllosilicates. In particular, when the inorganic part has a talc structure, that is, with Si atoms in the tetrahedral sheets and Mg atoms in the octahedral sheets, these compounds are named talc-like hybrids (TLHs). Properties of TLHs can easily be tailored by choosing the appropriate organoalkoxysilane as a silicon source. For example, using aminopropyltrimethoxysilane leads to materials with heavy-metal retention properties.[8]

In our work,[9] phenylaminomethyltrimethoxysilane (PAM) and phenethyltrimethoxysilane (PE) were chosen as silicon sources to prepare new TLHs for applications in the field of clay/polymer nanocomposites. Indeed, the presence of the aromatic groups is expected to enhance the compatibility between polymers, such as styrene, and the TLHs. It was shown that the inorganic part of these materials possesses a lamellar structure. Furthermore FTIR and ^{13}C MAS NMR spectroscopies proved the integrity of the organic moieties in the interlayer space. Due to differential thermal gravimetric analysis (TG-DTA), chemical analysis, and ^{29}Si MAS NMR spectroscopy, a chemical formula was proposed for both PAM-TLH $\{(Na_{0.13}Mg_{2.98}(RSi)_{3.96}[O_{6.10}(OH)_{5.78}]$; R = $PhNHCH_2\}$ and PE-TLH $Na_{0.18}Mg_{2.86}(RSi)_{4.03}[(O_{8.32}OH)_{1.36}]$; R = $Ph(CH_2)_2\}$. The aim of this work is to investigate whether the presence of organic moieties covalently linked to Si atoms has an influence on the structural arrangement of the Mg atoms located in the octahedral sheet. For this purpose, X-ray Absorption spectroscopy is a powerful tool to characterize the local order of a specific element in a material (Mg in the present case). The X-ray absorption near-edge structure (XANES) spectra generally show several peaks in which the positions and intensities are related to specific chemical bonds; the comparison of the observed spectra to data from reference materials yields useful information. In the present work, a comparison between the XANES spectra recorded from TLHs and

[a] Equipe Matériaux à Porosité Contrôlée (MPC), Institut de Science des Matériaux de Mulhouse (IS2M, LRC CNRS 7228), Université de Haute-Alsace,
3, rue Alfred Werner, 68093 Mulhouse Cedex, France
[b] Equipe Mécanique Matériaux et Procédés de Fabrication (MMPF), Laboratoire de Physique, Mécanique, Textile (LPMT, EA 4365, conventionnée au CNRS), Université de Haute Alsace,
61 rue Albert Camus, 68093 Mulhouse Cedex, France
E-mail: marie-helene.tuilier@uha.fr
[‡] Present address: Institut Charles Gerhardt (UMR CNRS 5253), Université de Montpellier 2,
Case 1701, Place Eugène Bataillon, 34095 Montpellier Cedex 5, France

related oxides, such as MgO (rock salt lattice), brucite [$Mg(OH)_2$] (single octahedral layered hydroxide),[10] and synthesized montmorillonite (TOT phyllosilicate), is presented.[11,12]

The similarity of the peak positions in the XANES spectra of the above compounds is highlighted. Very little theoretical data on the electronic structure of phyllosilicates with distorted Mg sites are available in the literature. Fortunately, the electronic structure of MgO, in which Mg is in regular octahedral coordination, has been extensively studied. Various theoretical approaches have been developed for an accurate interpretation of XANES and electron energy loss near-edge structures (ELNES), namely, multiple scattering simulations,[13] band structure,[14] and molecular cluster calculations.[15–16] These approaches are discussed and used for the interpretation of our data. In addition, Mg–O bond lengths are derived from Extended X-ray absorption fine structure (EXAFS) analyses of the PAM- and PE-TLH hybrids.

Results and Data Analysis

Structural Considerations

To begin with, it is interesting to focus on the parent structure of our TLHs. The simplest related structure is MgO, in which the Mg cation has six oxygen neighbors at $a/2$ = 2.105 Å and 12 second Mg neighbors at $a\sqrt{2}/2$ = 2.98 Å. One step further is brucite, whose structure consists of octahedral sheets of Mg with OH groups orthogonal to the hexagonal basal plane. In this compound, the Mg–O bond length is 2.10 Å, as in MgO. The phyllosilicate structure is related to the one of brucite, indeed the octahedral sheet is sandwiched between silicon tetrahedral sheets. In talc, octahedral sheets contain only Mg, whereas in montmorillonite Al is also present. In talc and montmorillonite, two sites (M1 and M2) are identified for metallic cations[17] (Figure 1). The mean metal–oxygen first distances for montmorillonite are 2.15 and 1.91 Å for M1 and M2, respectively (Figure 1, a). The Al–O and Mg–O distances derived from a previous EXAFS investigation of synthetic montmorillonite[11,12] revealed that the Al and Mg atoms in the octahedral sheet have different coordination radii with values of 1.93 and 2.13 Å, respectively. This result is consistent with the values of the ionic radii of Al and Mg, which lead to 1.96 and 2.10 Å for the Al–O and Mg–O bonds, respectively. Therefore, Mg should be located at M1 and Al at M2. The local environment of the metallic atoms in the octahedral sheet of the ideal structure of talc is roughly similar to montmorillonite, except that both the M1 and M2 sites should have two short M–O bonds (ca. 1.90 Å) and four longer M–O bonds (ca. 2.15 Å)[18] as displayed in Figure 1.

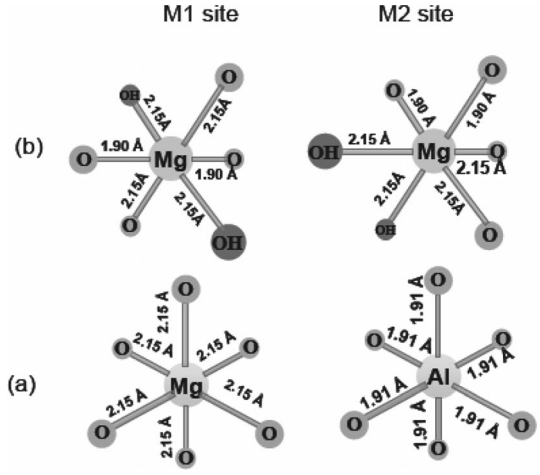

Figure 1. (a) The M1 crystallographic site of Mg and the M2 site of Al in montmorillonite according to ref.[20] and (b) M1 and M2 crystallographic sites of Mg in talc according to ref.[18]

Results on Mg *K*-Edge X-ray Absorption Spectroscopy

The Mg *K*-edge EXAFS spectra of PE-TLH and PAM-TLH are presented in Figure 2, together with that of montmorillonite and MgO. From the bottom of the absorption edge at 1306 eV, three peaks, A, B, and C, are observed in the near-edge region for the montmorillonite sample. The energy positions of the peaks are determined to within 0.2 eV and summarized in Table 1, together with brucite data taken from the literature.[19] Three resonances appear, at the same approximate energies, in the MgO near-edge spectrum (Figure 2); the intense and narrow edge line at 1309.4 eV (peak A), and a double-peaked resonance with maxima at 1314.8 and 1317.2 eV (peaks B and C, respectively). The resolution of the Mg *K*-edge spectra decreases in the following order: MgO > montmorillonite > $Mg(OH)_2$[19] > PE-TLH > PAM-TLH. It is interesting to note that the peaks are quite smooth in the PAM-TLH and PE-TLH spectra but the energy position of peak B is similar to that of montmorillonite. It is also noteworthy that the spectrum of synthetic montmorillonite is better resolved than that of natural montmorillonite with approximately the same composition.[20] The XANES region, above 1325 eV, consists of a broad feature (peak D) with peaks at 1330 eV in the hybrids and 1332 eV in montmorillonite.

The EXAFS data analysis was performed by using the IFEFFIT interactive software.[21] First, the oscillating part of the absorption spectra was extracted through the ATHENA routine. The E_0 origin of the kinetic energies of the photoelectron was taken at 1307.6 eV for all the samples. The experimental χ(k) spectra of PE-TLH and PAM-TLH are shown in Figure 3 (a). After conversion to k-space, in which k is the wave vector of the photoelectron scattering on the neighboring atoms, the data were k^1-weighted and Fourier transformed between 2.2 and 7.2 $Å^{-1}$. The Fourier transforms (FT) of the experimental spectra are presented in Figure 3 (b). The Mg atom nearest and next-nearest neighbor distributions of PAM-TLH (solid

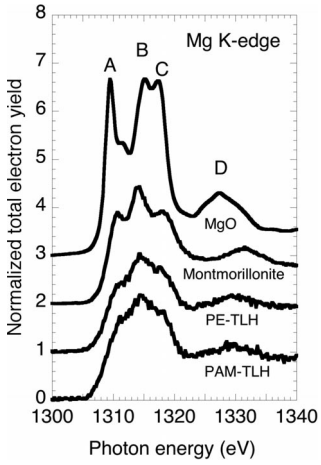

Figure 2. Near Mg *K*-edge XANES spectra of PAM-TLH, PE-TLH (recorded in fluorescence yield mode), synthetic montmorillonite, and MgO (recorded in total electron yield mode).

Table 1. Energy positions of the resonances observed in the near-edge spectra of the samples. The values in brackets indicate shoulders.

Sample	Peak A (eV)	Peak B (eV)	Peak C [eV]
MgO	1309.4	1314.8	1317.2
Synthetic montmorillonite	1310.7	1314.2	1318.1
Brucite $Mg(OH)_2$ [a]	(1312)	1315	(1319)
PE-TLH	–	1314.5	–
PAM-TLH	–	1314.5	–

[a] Taken from ref.[19]

line) are significantly shifted towards longer distances with respect to those of PE-TLH data (dashed line). The narrow range of the EXAFS spectra prevents the use of sophisticated structural models to fit the data of those complex materials using ARTEMIS. Thus the simulations are only performed on the nearest neighbor distribution. Let us recall that in theoretical talc structures,[18] the Mg atoms are shared between two M1 and M2 sites, which are quite equivalent to within the accuracy of the EXAFS technique. The theoretical difference between Mg–O_1 and Mg–O_2 (0.25 Å, see above) should lead to a beat node around 6.3 $Å^{-1}$, which is not observed in the experimental EXAFS data. Consequently, Mg–O_1 and Mg–O_2 bond lengths are closer together. These considerations led us to estimate first the average Mg–O distance by simply using an FEFF calculation[22] performed by using the coordinates of the O atoms around the Mg in MgO. The damping of the Fourier filtered contribution, however, was not well reproduced by the one shell fit. Beyond that first approach, an attempt to refine the model was carried out by running FEFF with an input file consisting of the coordinates of the O atoms around Mg in the M1 site of the theoretical talc structure (see above).[18] The values of Debye–Waller parameters (σ^2) were kept constant and both equal to 0.001 in the two-shell fits. The results of the calculations are summarized in Table 2. The two-shell fit curves are presented in the R-space in Figure 4 (solid lines). The degrees of degeneracy of Mg–O_1 and Mg–O_2 sub-shells are 2 and 4, respectively. The quality of the simulations is improved with respect to the one-shell fit. The weighted average of the bond lengths (2.13 and 2.18 for PE-TLH and PAM-TLH, respectively) is consistent with the results obtained within the one-shell approach.

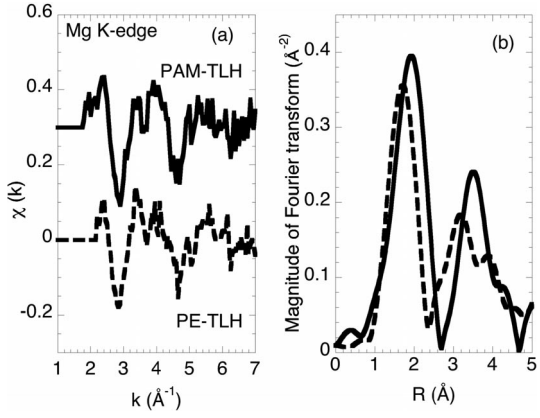

Figure 3. (a) Mg *K*-edge EXAFS spectra of hybrids and (b) the magnitudes of Fourier transforms of the k^1-weighted EXAFS data (uncorrected from phase shifts).

Table 2. Mg–O interatomic distances and Debye–Waller parameters derived from simulation of the nearest neighbour shells of hybrids.

Sample	One shell fit R_{Mg-O} [Å]	σ^2 [Å^2]	Two-shell fit R_{1Mg-O} [Å]	R_{2Mg-O} [Å]
PE-TLH	2.10 ± 0.05	0.01	2.02 ± 0.03	2.16 ± 0.03
PAM-TLH	2.16 ± 0.06	0.01	2.08 ± 0.03	2.23 ± 0.03

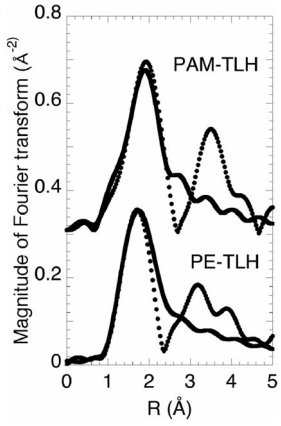

Figure 4. The magnitudes of Fourier transforms of nearest neighbor peaks of experiments (dots) and simulations (lines) using the parameters in Table 2 (two-shell fits).

Discussion

The *K*-edge EXAFS spectra of low Z elements is assigned to the transition of the 1s electrons to the unoccupied states with 3p character. For a better understanding of the *K*-edge spectra of the hybrids (Figure 2), it is interesting to focus our interest on oxides having sixfold coordinated

Mg atoms in simpler structures, such as brucite and MgO. It is well established from the study of Al *K*-edges in oxides[19,23] that materials with regular octahedral sites have a single white line. The intense near-edge resonance observed in the MgO EXAFS spectrum (peak A, Figure 2) should be due to the regular sixfold coordination. Various theoretical calculations including the core hole effect are available for MgO XANES and ELNES spectroscopy.[13–16,24] First, the multiple scattering calculations[13] performed with one shell of six regularly coordinated O atoms around the Mg absorber give rise to a sharp peak. This result has been understood as a caging effect of the O shell on the excited electron. Peak A becomes smoother in the spectra of montmorillonite and TLH due to the distortion of the Mg environment with respect to perfect octahedral coordination. Peaks B and C are obtained from molecular simulation (MS) calculations including six shells in an 80-atom MgO cluster, but this approach is unable to find the origin of peaks B and C, and to reproduce accurately their energy positions. The band structure (BS) calculations including core hole effect and a large cluster for the final-state calculation allow a rather satisfactory reproduction of the peak positions and their relative intensities.[14] In the latter approach, the local density of states (LDOS) is obtained from orthogonal linear combination of atomic orbitals (LCAO) within a DFT based on a BS method. In a recent work, Tcrera et al.[25] have reported Mg *K*-edge EXAFS spectra of various minerals and performed DFT calculations on diopside (in which the Mg atom has sixfold coordination).

On the other hand, the Mg *K*-edge EXAFS absorption spectrum of brucite[23] resembles those of PAM-TLH and PE-TLH. The spectrum features are less prominent in brucite than in montmorillonite (Table 1). The Mg *p*-density of states (DOS) of brucite has been calculated by using the ab initio all-electron LCAO Hartree–Fock model.[10] It presents a weak maximum at 0.2 Hartree (around 5.4 eV) and a main peak at 0.4 Hartree (around 11 eV). When taking into account the core hole effect that increases the energy of the levels, they correspond rather well to the edge shoulder A (4 eV above the bottom of the absorption edge) and the main peak B (8 eV), respectively.

Among the theoretical calculations developed in the last years for the interpretation of MgO XANES and ELNES, the molecular cluster calculation of Mizoguchi et al.[15,16] seems the most relevant for a better understanding of the electronic structure of oxides in which Mg is in more or less regular sixfold coordination. As a matter of fact, such an approach using orthogonal LCAO within DFT, and taking into account the core hole effects, describes, beyond the partial DOS, the interaction between the orbitals of the core-holed Mg atom (labeled Mg* in ref.[15]) and its surrounding atoms, thereby allowing an accurate assignment of peaks A, B, and C. The Mg and O atoms mainly exhibit antibonding interactions in the unoccupied bands, which is quite natural for ionic compounds.[15] The peaks A and C observed in the MgO XANES spectrum are assigned to bonding and antibonding interactions between Mg* p orbitals of the core-holed atom and Mg p orbitals of the neighbors, whereas peak B corresponds to Mg* *p*-Mg 1s. In summary, the main features of MgO XANES spectrum could be due to an Mg* p -Mg interaction. Due to the lack of calculations of XANES spectra for TOT phyllosilicates, it is interesting to note that the weaker intensity of the three peaks in montmorillonite and the hybrids with respect to MgO should be related to a lower Mg–Mg orbital overlap.

The EXAFS spectroscopic analysis is consistent with two different Mg–O distances being identified in the octahedral sheet of TLHs. The $Mg–O_1$ bonds (Table 2), however, are found to be significantly higher than predicted in the theoretical talc structure (about 1.90 Å for both M1 and M2 sites). This is not surprising if one sums the ionic radii of Mg^{2+} and O^{2-} (2.11 Å). The $Mg–O_1$ bonds could not be easily shortened to 0.2 Å below that value. Consequently, the difference between $Mg–O_1$ and $Mg–O_2$ (around 0.15 Å for both hybrids) is smaller than the value predicted in the theoretical talc structure (0.25 Å). The $Mg–O_2$ bond in PE-TLH is in fair agreement with the theoretical value (about 2.15 Å for both M1 and M2 sites). This value is found to be longer in PAM-TLH than in PE-TLH (Table 1). In the former, the phyllosilicate units are smaller than those in the latter, as attested by TEM micrographs.[9] As shown above, the nearest neighbor environment has little effect on the near-edge spectra. The main part of Mg–O bonds is longer in the hybrids than in MgO and montmorillonite, thus leading to a smaller overlap of Mg–Mg orbitals. It is not surprising that near-edge features are smooth, like in brucite, in which Mg–Mg interatomic distances are significantly lengthened with respect to MgO and montmorillonite.

The broad (060) XRD reflection observed for the PAM-TLH samples indicates a less homogeneous environment of the elements in the octahedral sheet.[9] Indeed, ^{29}Si MAS NMR spectroscopy revealed that the local environment of the Si atoms in the tetrahedral sheets of the hybrid materials is strongly affected by the nature of the organic species. Our previous work[9] showed that PE-TLH presents a majority of T^3 units, indicating a well-condensed tetrahedral sheet, whereas for PAM-TLH, the ^{29}Si MAS NMR spectrum exhibits mainly T^2 and T^1 units. The T^n units correspond to the number of OM (M = Si or Mg) connections that a silicon atom has, $Si(R)(OM)_n(OH)_{3-n}$ (R = PAM or PE) and informs about the degree of silicon condensation in the tetrahedral sheet. Consequently, the PAM-TLH sample presents a wider distribution of silicon environments (T^1 and T^2 units) than observed for PE-TLH (T^3). These results seem to indicate that the nature of the organoalkoxysilane has a strong influence on the condensation degree of the tetrahedral sheet, whereas the octahedral sheet of the hybrid materials is less affected.

Conclusion

The Mg *K*-edge XAFS spectra of TLHs, synthesized montmorillonite, and MgO show three main peaks. According to literature, *K*-edge XANES spectra give information on the unoccupied states with p character. It emerges from

the MgO band structure calculations that the intensity of near-edge features is related to the overlap of p orbitals belonging to Mg absorber atoms and their secondary neighbors. Consequently, XANES fingerprints of the different studied materials were used to appreciate the evolution of the overlap between the Mg–Mg orbitals depending on the linked organic moieties. The orbital overlap could explain the strength of the octahedral sheet in phyllosilicates. Moreover, the three peaks observed become smoother in the order MgO > montmorillonite > $Mg(OH)_2$ > PE-TLH > PAM-TLH, as the distortion of the Mg environment with respect to perfect octahedral coordination increases. The mean Mg–O bond length is close to 2.1 Å in all of the studied materials. But the deviation from the regular octahedral coordination is evidenced in hybrids, in which two different Mg–O distances are derived from the EXAFS analysis. This set of results highlights the noteworthy stability of the octahedral frame in the Mg-based phyllosilicates. This work underlines the interest of XAFS for the characterization of such complex hybrids materials and should stimulate theoretical work in such a field.

Experimental Section

Syntheses: Phenylaminomethyl and phenethyl talc-like hybrid materials (PAM-TLH and PE-TLH, respectively) were prepared by a one-step synthetic procedure described previously.[9] The procedure used for the synthesis of montmorillonite containing Mg is described in details in ref.[11,26]

The X-ray absorption experiments were performed at the Swiss Light Source, Paul Scherrer institute, Villigen, Switzerland, on the microfocus soft X-ray absorption LUCIA beam line.[27] The Mg *K*-edge EXAFS spectra were collected at r.t. using a KPT (potassium titanyl phosphate, $KTiOPO_4$) two-crystal monochromator, both in fluorescence mode and total electron yield (TEY) mode. TEY mode gives less noisy spectra, but the charge effect during the data acquisition leads to subsequent distortions of EXAFS baselines. The powdered samples were spread on a self-adhesive indium surface, which were then deposited onto a copper sheet. The beam was focused using a Kirkpatrick–Baez two mirror system onto the surface sample in a spot of about $5 \times 10\ \mu m^2$ diameter. The accumulation lasted about 10 s by 0.2 and 1 eV energy steps in the XANES and EXAFS regions, respectively. The description of the Mg *K*-edge XAFS experiments performed on synthesized montmorillonite and MgO reference samples is given in ref.[11]

Acknowledgments

The authors thank La Fondation pour l'Ecole Nationale Supérieure de Chimie de Mulhouse for financial support. The authors also would like to thank the staff of the SLS synchrotron at Villigen, especially Dr D. Vantelon, Dr P. Lagarde (LUCIA beam line), for their help. The authors are grateful to the machine and beam line groups whose outstanding efforts have made these experiments possible. Dr G. Arnold and M. Gîrleanu are acknowledged for contributing to the XAFS experiments.

[1] L. Betega de Paiva, A. R. Morales, F. R. Valenzuela Diaz, *Appl. Clay Sci.* **2008**, *42*, 8–24.
[2] A. R. McLauchlin, N. L. Thomas, *J. Colloid Interface Sci.* **2008**, *321*, 39–43.
[3] K. A. Carrado, L. Xu, R. Csencsits, J. V. Muntean, *Chem. Mater.* **2001**, *13*, 3766–3773.
[4] J. H. Joo, J. H. Shim, J. H. Choi, C. H. Choi, D.-S. Kim, J.-S. Yoon, *J. Appl. Polym. Sci.* **2008**, *109*, 3645–3650.
[5] Y. Fukushima, M. Tani, *J. Chem. Soc., Chem. Commun.* **1995**, 241–242.
[6] M. G. D. Fonseca, C. Airoldi, *J. Chem. Soc., Dalton Trans.* **1999**, 3687–3692.
[7] B. Lebeau, N. T. Whilton, S. Mann, *Mater. Res. Soc. Symp. Proc.* **2002**, 726–735.
[8] M. Jaber, J. Miehé-Brendlé, L. Michelin, L. Delmotte, *Chem. Mater.* **2005**, *17*, 5275–5281.
[9] J.-C. Gallégo, M. Jaber, J. Miehé-Brendlé, C. Marichal, *New J. Chem.* **2008**, *32*, 407–412.
[10] P. D'Arco, M. Causa, C. Roetti, B. Silvi, *Phys. Rev. B* **1993**, *47*, 3522–3529.
[11] M. Reinholdt, J. Miehé-Brendlé, L. Delmotte, M.-H. Tuilier, R. l. Dred, R. Cortès, A.-M. Flank, *Eur. J. Inorg. Chem.* **2001**, *11*, 2831–2841.
[12] M. Reinholdt, *PhD Thesis*, Mulhouse, France, **2001**.
[13] Th. Lindner, H. Sauer, W. Engel, K. Kambe, *Phys. Rev. B* **1986**, *33*, 22–24.
[14] S.-D. Mo, W. Y. Ching, *Phys. Rev. B* **2000**, *62*, 7901–7907.
[15] T. Mizoguchi, I. Tanaka, *Phys. Rev. B* **2000**, *61*, 2180–2187.
[16] T. Mizoguchi, K. Tatsumi, I. Tanaka, *Ultramicroscopy* **2006**, *106*, 1120–1128.
[17] S. I. Tsipursky, V. A. Drits, *Clay Miner.* **1984**, *19*, 177–193.
[18] J. W. Gruner, *Z. Kristallographie* **1934**, *88*, 412–419.
[19] J. A. v. Bokhoven, J. C. A. A. Roelofs, K. d. Jong, D. C. Koningsberger, *Chem. Eur. J.* **2001**, *7*, 1258–1265.
[20] D. Li, M. Peng, T. Murata, *Can. Mineral.* **1999**, *37*, 199–206.
[21] B. Ravel, M. Newville, *J. Synchrotron Radiat.* **2005**, *12*, 537–541.
[22] S. I. Zabinsky, J. J. Rehr, A. Ankudinov, R. C. Albers, M. J. Eller, *Phys. Rev. B* **1995**, *52*, 2995–3009.
[23] J. A. v. Bokhoven, H. Sambe, D. E. Ramaker, D. C. Koningsberger, *J. Phys. Chem. B* **1999**, *103*, 7557–7564.
[24] S. Köstlmeier, C. Elsässer, *Phys. Rev. B* **1999**, *60*, 14025–14034.
[25] N. Trcera, D. Cabaret, S. Rossano, F. Farges, A.-M. Flank, P. Lagarde, *Phys. Chem. Miner.* **2009**, *36*, 241–257.
[26] M. Reinholdt, J. Miehe-Brendle, L. Delmotte, R. Le Dred, M.-H. Tuilier, *Clay Miner.* **2005**, *40*, 177–190.
[27] A.-M. Flank, G. Cauchon, P. Lagarde, S. Bac, M. Janousch, R. Wetter, J.-M. Dubuisson, F. L. M. Idir, T. Moreno, D. Vantelon, *Nucl. Instrum. Methods Phys. Res., Sect. B* **2006**, *246*, 269–274.

Received: February 24, 2010
Published Online: November 3, 2010

